

Radiative electron attachment to rotating C₃N through dipole-bound states

Joshua Forer^{1,2}, Viatcheslav Kokoouline¹, Thierry Stoecklin²

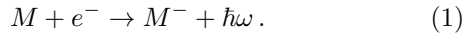
¹*Department of Physics, University of Central Florida, Orlando, Florida 32816, USA*

²*Institut des Sciences Moléculaires, Université de Bordeaux,
CNRS UMR 5255, 33405 Talence Cedex, France*

(Dated: November 14, 2022)

The role of a large dipole moment in rotating neutral molecules interacting with low-energy electrons is studied using an accurate *ab initio* approach accounting for electronic and rotational degrees of freedom. It is found that theory can reproduce weakly-bound (dipole-bound) states observed in a recent photodetachment experiment with C₃N⁻ [Phys. Rev. Lett. **127**, 043001 (2021)]. Using a similar level of theory, the cross section for radiative electron attachment to the C₃N molecule, forming the dipole-bound states, was determined. The obtained cross-section is too small to explain the formation of C₃N⁻ in the interstellar medium, suggesting that it is likely formed by a different process.

Introduction Despite the large amount of molecules detected in interstellar and circumstellar environments, only six molecular anions have been detected [1–5]: CN⁻, C₃N⁻, C₅N⁻, C₄H⁻, C₆H⁻, and C₈H⁻. Their formation is not yet well understood. Initially, it was proposed that such anions are formed by the process of radiative electron attachment (REA), in which a free electron can attach to the neutral molecule M and release excess energy via photon emission



However, previous calculations [6–9] have shown that REA rates are too low to explain the observed abundance of CN⁻, C₃N⁻, and C₅N⁻. It was then suggested that the REA mechanism could take place via a “doorway” weakly bound dipole state (DBS) [10], first described by Fermi and Teller in 1947 [11]. For a point dipole interacting with a charge, the existence of an infinite number of DBSs was predicted for dipole values larger than a critical value of approximately 0.65 a.u. [12] (a.u. here and below are atomic units). Including additional molecular effects, however, modifies this value while reducing the number of DBSs to just a few. Other contributions to the long-range potential being associated with the electrostatic and polarization potentials need to be considered when modeling a neutral polar molecule interacting with a point charge and, for these reasons, some authors have also investigated the possible existence of quadrupole and polarization bound states [13, 14]. Experimentally, the minimum dipole moment required for the formation of stable dipole-bound anions of common closed-shell molecules has been measured to range between 2–2.5 D. Over the years, the effect of vibration [15] and rotation of the dipolar molecule on the DBS was also investigated [16, 17], showing that the critical moment for a rotating dipole is larger than that of a stationary dipole. However, a quantum study of REA through a dipole-bound state including both the rotation of the molecule and the short range part of the electron-molecule poten-

tial is missing. In this study we consider the REA process via the DBSs of one of the anions detected in the ISM: C₃N⁻. This molecule is a good candidate because the C₃N dipole is supercritical and the existence of a C₃N⁻ DBS was demonstrated in a recent ion trap experiment. [10]

Theoretical model The theoretical model of the present study is based on wave functions (bound and continuum states) of the e⁻-C₃N system obtained by solving the Schrödinger equation. The potential energy operator of the e⁻-C₃N system is calculated in the molecular center-of-mass frame with the \hat{z} -axis directed along the molecular axis, pointing towards the N atom, while the incident electron’s polar coordinates in this frame are denoted by (r, θ) . To highlight the effect of the short range contribution, two different potentials will be used. The first potential, V_{dip} , is restricted to only the long-range interaction between a point charge and a dipole

$$V_{\text{dip}} = -\frac{\mu e}{r^2} P_1(\cos \theta), \quad (2)$$

where μ is the dipole moment of C₃N ($\mu = 1.3$ a.u.) and $P_1(\cos \theta)$ is a Legendre polynomial.

The second interaction potential V_{ai} between neutral C₃N and the impinging electron is an *ab initio* potential made of four contributions and obtained as a function of the electronic wave function ψ^e of C₃N

$$V_{\text{ai}}(\psi^e) = V_{\text{Stat}}^e(\psi^e) + V_{\text{nuc}} + V_{\text{Ex}}^{\text{HFEGE}}(\psi^e) + V_{\text{copol}}(\psi^e), \quad (3)$$

where $V_{\text{Stat}}^e(\psi^e)$ is the electronic part of the static potential, V_{nuc} is the contribution of the nuclear potential, and the two remaining terms are exchange and correlation-polarization contributions, respectively. The latter two contributions are obtained in the usual density-functional forms of Morrison and Collins [18] and Padial and Norcross [19]. The perpendicular α_{\perp} and parallel α_{\parallel} polarizabilities, and the ionization potential of C₃N, needed for the potential of Eq.(3), are 27.11, 60.35, and 0.53 a.u., respectively. The ground electronic state ($X^2\Sigma^+$) wave

function of C_3N , ψ^e , is calculated for its equilibrium geometry. At equilibrium, the molecule is linear with the following three internuclear distances in the C-C-C-N arrangement: 2.30, 2.62, and 2.13 a.u., respectively (see the supplementary material of Ref. [9]). The same geometry is used within the fixed nuclei approximation for performing the *ab initio* and REA calculations as well as those of the $C_3N^-(X^1\Sigma^+)$ bound states within the rigid rotor approximation. The *ab initio* calculations are performed with the MOLPRO [20] software suite at the MCSCF level and using the `aug-ccpV6Z(d)` atomic orbital basis [21]. The obtained dipole moment of C_3N of 1.3 a.u. is in very good agreement with the CAS-CI value 1.4 a.u. by Harrison and Tennyson [22], suggesting that the main contribution to the long-range e^-C_3N potential is well described at this level of theory.

In order to obtain the potential as a series of Legendre polynomials

$$V_{ai} = \sum_{\lambda=0,80} C_{\lambda}(r)P_{\lambda}(\cos\theta) \quad (4)$$

the *ab initio* multi-centered gaussian basis set is first analytically shifted and expanded around the centre of mass in a symmetrized, real spherical harmonics basis set [23] for values of l up to 380. From this development, analytical Legendre polynomial expansion-coefficients of the electronic potential $V_{Stat}^e(\psi^e)$ — by far the strongest contribution — are obtained using the standard procedure [24].

Figure 1 compares the two potentials. The potentials are significantly different at small distances, demonstrating that the point dipole potential may not accurately describe the C_3N DBS. The V_{ai} potential accounts for the short- and long-range contributions. The nuclear potential V_{nuc} is strongly attractive near the nuclei where it dominates all the other contributions. For larger, but not very large, values of r , the sum of the repulsive electronic potential and the attractive exchange and correlation-polarization contributions makes the overall potential less attractive than the pure charge-dipole potential V_{dip} . We do not expect high-energy continuum states and resonances to be accurately represented by the V_{ai} potential, but it should describe the process well, qualitatively, at low collision energies where the balance between the long- and mid-range potential controls the dynamics.

Dipole-bound states The close-coupling method is used to solve the Schrödinger equation for bound and continuum states using the Magnus propagator within the Newmat code as detailed in a previous study [25]. The calculations included 40 rotational states of C_3N and were propagated from $r = 0.1$ to 300 a.u. while the boundary between propagation and counter-propagation was fixed at 3.2 a.u. DBS energies obtained for the two potentials and different values of total angular momentum J are

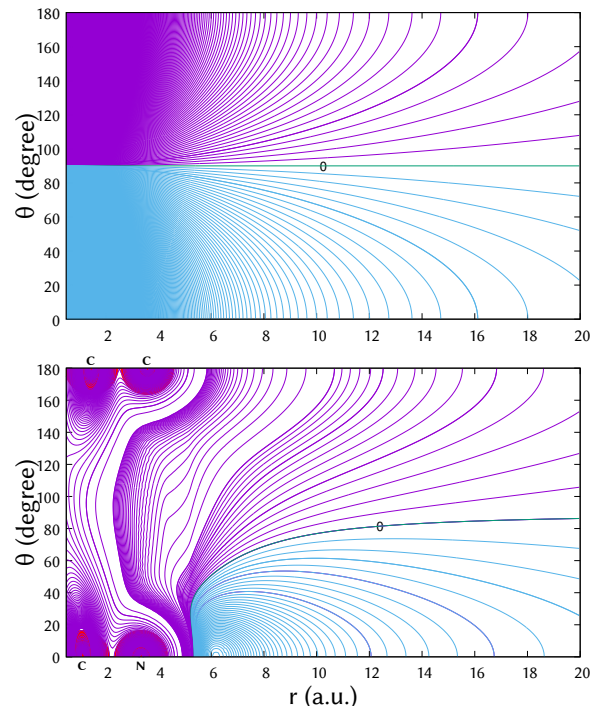


FIG. 1: The two potentials used in the study, V_{dip} (upper panel) and V_{ai} (lower panel), shown as a function of the Jacobi coordinates r and θ . The energy-dependent potential V_{ai} is represented at an electron scattering energy -0.1 eV (~ 806.5 cm^{-1}). The origin of the figure is the C_3N center of mass. The positions of the four atoms are also reported.

given in Table I.

The potential V_{dip} has bound states up to $J = 11$, while V_{ai} only supports bound states up to $J = 5$. This difference results from the less attractive mid-range part of V_{ai} compared to V_{dip} . In both cases, the only possible states with $J > 0$ have odd parity if J is even, and even parity if J is odd. The spacing between successive levels in both cases follows the usual law for a linear molecule with a rotational constant of C_3N^- , which is very close to the one of C_3N (0.16504 cm^{-1} [26]). The $J = 0$ bound-state energy obtained with the pure charge-dipole potential V_{dip} is quite large when compared to the experimental value (-2 ± 1 cm^{-1}) of Wester [10]. The corresponding value for V_{ai} is closer to the experiment but still three times larger. If we take into account (1) the experimental temperature of the ion trap (16 K), which allows populating several rotationally-excited dipole bound states, and (2) the energies computed with V_{ai} , we obtain a Boltzmann-average peak position in the photodetachment spectrum of -3.8 cm^{-1} , which is in good agreement with its experimental estimate. The agreement within a few cm^{-1} with the theoretical value, obtained neglecting rotation by Jerosimić *et al.* [27] (-2 cm^{-1}) from an MRCI calculation of C_3N^- , is also satisfactory and demonstrates

J	$E(V_{\text{ai}})$	$E(V_{\text{dip}})$
0	-6.87	-22.13
1	-6.57	-21.80
2	-5.87	-21.14
3	-4.90	-20.15
4	-3.51	-18.84
5	-1.87	-17.19
6		-15.21
7		-12.91
8		-10.27
9		-7.30
10		-4.01
11		-0.38

TABLE I: DBS energies (cm^{-1}) obtained for the two potentials for different values of J .

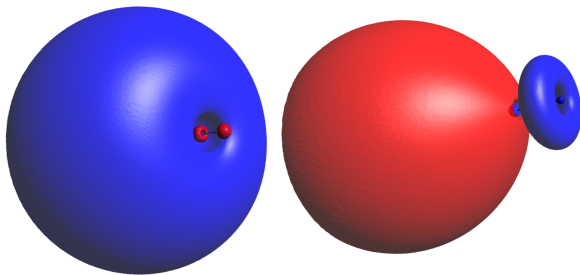


FIG. 2: Dipole-bound states of C_3N^- for $J = 0$ with energy -6.87 cm^{-1} (left) and $J = 1$ with energy -6.57 cm^{-1} (right)

the validity of the V_{ai} potential.

Figure 2 shows two examples of DBS wave functions obtained for the V_{ai} potential for $J = 0$ with energy -6.87 cm^{-1} and $J = 1$ with energy -6.57 cm^{-1} . The DBS wave functions with higher J qualitatively look the same but have additional nodes along the \hat{z} -axis. Additionally, wave functions obtained with the V_{dip} potential have the same behavior as the ones obtained with V_{ai} at large values of r , but have fewer features with small amplitudes at short distances due to the simpler behavior of V_{dip} in this region (see Fig. 1).

Electron-molecule scattering and radiative attachment For REA calculations, e^- - C_3N continuum-state wave functions are also needed. A key difference between our approach and that of Lara-Moreno *et al.* [8] is that the effect of rotation on the REA process is accounted for. The space-fixed frame is then more appropriate than the body-fixed frame used in that previous study. We furthermore take advantage of using a local model of the e^- - C_3N potential and use a method initially developed for radiative association [28, 29] and later adapted to REA [30, 31].

We do not resolve molecular vibration and write the rigid rotor scattering wave function of the system in Jacobi coordinates in the following form

$$\psi^i(\vec{r}, \hat{Z}) = \frac{1}{r} \sum_{jl} \chi_{jl}^{JM}(r) Y_{jl}^{JM}(\hat{r}, \hat{Z}), \quad (5)$$

where \vec{r} and \hat{Z} are respectively the electron coordinate vector and the orientation angles of the C_3N axis in the space-fixed frame. The indices j and l are, respectively, the C_3N rotational and electron orbital quantum numbers, while the total angular momentum of the system is $\vec{J} = \vec{j} + \vec{l}$. The $Y_{jl}^{JM}(\hat{R}, \hat{r})$ angular functions take the usual form

$$Y_{jl}^{JM}(\hat{r}, \hat{Z}) = \sum_{m_j m_l} \langle j m_j l m_l | J M \rangle Y_k^{m_l}(\hat{r}) Y_j^{m_j}(\hat{Z}), \quad (6)$$

where M , m_j , and m_l are, respectively, the projections of \vec{J} , \vec{j} , and \vec{l} on the space-fixed \hat{z} -axis.

For a given value of J , the radial part of the scattering wave function $\chi_{jl}^J(r)$ is the solution of the driven differential equation [29]

$$\left(\frac{d^2}{dr^2} - \frac{l(l+1)}{r^2} + k_j^2(E) - 2m_r U_{j'l',jl}^J(r) \right) \chi_{j'l',jl}^J(r) = \lambda_{jl}^{\alpha J}(r) \quad (7)$$

where $U_{j'l',jl}^J(r)$ is the potential matrix in basis set (6). The right-hand-side term is called the driving term for a given initial state of the e^- - C_3N system and final state of C_3N^- , each respectively characterized by the sets of quantum numbers (j, l) and (α, J') . It is real-valued and results from the dipolar coupling of the initial (scattering) and final (bound) states within the dipolar approximation. It is given by

$$\lambda_{jl}^{\alpha J}(r) = -2m_r \int d\hat{r} d\hat{Z} Y_{jl}^{JM}(\hat{r}, \hat{Z}) \mu(\vec{r}, \hat{Z}) \psi_{\alpha J'}^f(\vec{r}, \hat{Z}), \quad (8)$$

where m_r is the reduced mass of the system. The final DBS functions $\psi_{\alpha J'}^f(\vec{r}, \hat{Z})$, presented in the previous section, were also calculated in the space fixed frame and expanded in the basis given by equation (6), i.e.,

$$\psi_{\alpha J'}^f(\vec{r}, \hat{Z}) = \frac{1}{r} \sum_{j'l} \omega_{j'l}^{J'M'}(r) Y_{j'l}^{J'M'}(\hat{r}, \hat{Z}). \quad (9)$$

The two sets of DBSs obtained using the potentials V_{ai} and V_{dip} are then used to calculate the REA cross section with a rotational basis of 40 states. The REA cross section is given by the following equation

$$\sigma_f^{\text{REA}} = \frac{g_a}{g_n} \frac{8\pi^2}{3k_e^2 c^3} \sum_{J, J', \alpha} \omega_{\alpha}^3 |M_{j, J'}^{\alpha J'}|^2, \quad (10)$$

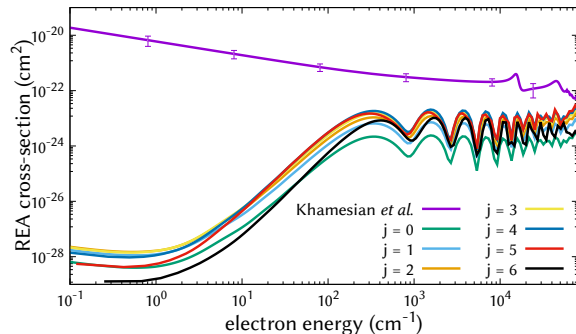


FIG. 3: The REA cross sections for different initial rotational states j of C_3N^- using the V_{ai} potential. The figure shows the result (purple curve) of the previous REA study [6]. The error bars on the curve represent the uncertainty of the model used in that study.

where the transition dipole moment $M_{j,J}^{\alpha,J'}$ is obtained from the driving term [29], g_a and g_n are respectively the degeneracy factors of the anion and the neutral, and ω_α is the frequency of the emitted photon.

Results Figure 3 shows the REA cross section for different initial rotational states j of C_3N using the V_{ai} potential. The cross section is summed over all possible final DBS states, i.e. over different J . The cross section for $j = 0$ is 2-4 times smaller than for larger values of j . At very small energies, below 1 cm^{-1} , the cross section is inversely proportional to the collision energy, as expected from Eq. (10). Between 1 and 100 cm^{-1} , it increases rapidly as, approximately, the square of the collision energy due to the ω_α^3/k_e^2 factor in Eq. (10). Above 100 cm^{-1} , the cross section oscillates due to the same behaviour of the transition dipole moment in Eq. (10), which varies due to the change in position of nodes in the initial continuum wave functions with the energy.

The figure also shows the result of the previous REA study [6], in which the REA cross section for transitions to the ground electronic state of C_3N^- were considered. At energies below 1 eV, the present cross sections are much smaller than the one in Ref. [6]. This is expected for low collision energies because the overall magnitude of the REA cross sections is governed by the ω_α^3 factor in Eq. (10), which is much smaller for transitions to DBSs than to ground electronic state of C_3N^- . The C_3N affinity is $\sim 34727 \text{ cm}^{-1}$ [10]. The cross sections approach the one obtained by Khamesian *et al.* [6], approximately, only at scattering energies that are larger than the C_3N^- affinity.

In their study, Khamesian *et al.* [6] concluded that the obtained REA cross section is too small to explain the observed abundance of C_3N^- ions in the ISM by formation via REA. In the present study, REA cross sections are even (significantly!) smaller at energies relevant for the interstellar medium. This means that the idea [33] that DBSs can increase the REA cross section and possi-

bly explain the observed abundance of C_3N^- by REA to C_3N should be abandoned.

Concluding, we would like to stress the following findings of the present study. Energies of dipole-bound states of rotating C_3N^- molecular ion were obtained using an accurate computational approach. In total, six weakly-bound states were found for $J = 0 - 5$. Cross sections for radiative attachment to the C_3N molecule forming the weakly-bound states of C_3N^- were obtained for several initial rotational states $j = 0 - 6$ of the neutral molecule and for a large interval of collision energies. The obtained REA cross sections are significantly smaller than those previously obtained for the process towards the ground electronic state of C_3N^- , which was, in principle, expected.

- It was concluded that the C_3N^- abundance observed in the ISM cannot be explained by formation of these ions by REA towards weakly or deeply bound electronic states of the ion. The present results obtained at the rigid rotor level suggest that the effect of the formation of long-lived resonances via vibrationally excited bending vibrations should be considered in future studies. The alternative formation mechanism of large molecular anions via reactions of carbon anions with N atoms should also be considered for C_3N^- as suggested by Bierbaum [34] and Agúndez *et al.* [35]. Five other negative ions observed in the ISM: CN^- , C_5N^- , C_4H^- , C_6H^- , and C_8H^- , deserve separate studies of this kind, as their formation mechanisms are probably not the same.
- A technical result, important for theorists: we have found that the short-range part of the electron-molecule interaction significantly influences the REA cross sections for energies below a few eV.
- The present approach can be applied to study weakly-bound states and electron scattering for systems where the strong quadrupole interaction is dominant at large distances, such as TCNB^- [36].

ACKNOWLEDGEMENTS

This work acknowledges the support from the National Science Foundation, Grant No.2110279, and the Fulbright-University of Bordeaux Doctoral Research Award.

[1] P. Thaddeus, C. A. Gottlieb, H. Gupta, S. Brünken, M. C. McCarthy, M. Agúndez, M. Guélin, and J. Cernicharo, Laboratory and astronomical detection of the

- negative molecular ion c_3n^- , *Astrophys. J.* **677**, 1132 (2008).
- [2] J. Cernicharo, M. Guélin, M. Agúndez, K. Kawaguchi, M. McCarthy, and P. Thaddeus, Astronomical detection of c_4H^- , the second interstellar anion, *Astron. Astrophys.* **467**, L37 (2007).
- [3] J. Cernicharo, M. Guélin, M. Agúndez, M. C. McCarthy, and P. Thaddeus, Detection of c_5nm and vibrationally excited c_6h in $irc +10216$, *Astrophys. J.* **688**, L83 (2008).
- [4] M. C. McCarthy, C. A. Gottlieb, H. Gupta, and P. Thaddeus, Laboratory and astronomical identification of the negative molecular ion c_6h^- , *Astrophys. J.* **652**, L141 (2006).
- [5] S. Brünken, H. Gupta, C. A. Gottlieb, M. C. McCarthy, and P. Thaddeus, Detection of the carbon chain negative ion c_8h^- in $tmc-1$, *Astrophys. J.* **664**, L43 (2007).
- [6] M. Khamesian, N. Douguet, S. Fonseca dos Santos, O. Dulieu, M. Raoult, W. J. Brigg, and V. Kokoouline, Formation of CN^- , C_3N^- , and C_5N^- molecules by radiative electron attachment and their destruction by photodetachment, *Phys. Rev. Lett.* **117**, 123001 (2016).
- [7] S. Harrison and J. Tennyson, Bound and continuum states of molecular anions c_2h^- and c_3n^- , *J. Phys. B.* **44**, 045206 (2011).
- [8] M. Lara-Moreno, T. Stoecklin, P. Halvick, and J.-C. Loison, Single-center approach for photodetachment and radiative electron attachment: Comparison with other theoretical approaches and with experimental photodetachment data, *Phys. Rev. A* **99**, 033412 (2019).
- [9] M. Lara-Moreno, T. Stoecklin, and P. Halvick, Radiative electron attachment and photodetachment rate constants for linear carbon chains, *ACS Earth and Space Chemistry* **3**, 1556 (2019).
- [10] M. Simpson, M. Nötzold, T. Michaelsen, R. Wild, F. A. Gianturco, and R. Wester, Influence of a supercritical electric dipole moment on the photodetachment of c_3n^- , *Phys. Rev. Lett.* **127**, 043001 (2021).
- [11] E. Fermi and E. Teller, The capture of negative mesotrons in matter, *Phys. Rev.* **72**, 399 (1947).
- [12] O. H. Crawford, Bound states of a charged particle in a dipole field, *Proc. Phys. Soc.* **91**, 279 (1967).
- [13] C. Desfrancois, H. Abdoul-Carime, N. Khelifa, and J. P. Schermann, From $\frac{1}{r}$ to $\frac{1}{r^2}$ potentials: Electron exchange between rydberg atoms and polar molecules, *Phys. Rev. Lett.* **73**, 2436 (1994).
- [14] Abdoul-Carime, H. and Desfrancois, C., Electrons weakly bound to molecules by dipolar, quadrupolar or polarization forces, *Eur. Phys. J. D* **2**, 149 (1998).
- [15] Č. S. Anstöter, G. Mensa-Bonsu, P. Nag, M. c. v. Ranković, R. Kumar T. P., A. N. Boichenko, A. V. Bochenkova, J. Fedor, and J. R. R. Verlet, Mode-specific vibrational autodetachment following excitation of electronic resonances by electrons and photons, *Phys. Rev. Lett.* **124**, 203401 (2020).
- [16] E. A. Brinkman, S. Berger, J. Marks, and J. I. Brauman, Molecular rotation and the observation of dipole-bound states of anions, *J. Chem. Phys.* **99**, 7586 (1993).
- [17] D. A. Walthall, J. M. Karty, and J. I. Brauman, Molecular rotations and dipole-bound state lifetimes, *J. Phys. Chem. A* **109**, 8794 (2005), PMID: 16834282.
- [18] M. A. Morrison and L. A. Collins, Exchange in low-energy electron-molecule scattering: Free-electron-gas model exchange potentials and applications to $e-h_2$ and $e-n_2$ collisions, *Phys. Rev. A* **17**, 918 (1978).
- [19] N. T. Padial and D. W. Norcross, Parameter-free model of the correlation-polarization potential for electron-molecule collisions, *Phys. Rev. A* **29**, 1742 (1984).
- [20] H.-J. Werner, P. J. Knowles, G. Knizia, F. R. Manby, M. Schütz, *et al.*, Molpro, version 2012.1, a package of ab initio programs (2012), see <http://www.molpro.net>.
- [21] A. K. Wilson, T. van Mourik, and T. H. Dunning, Gaussian basis sets for use in correlated molecular calculations. vi. sextuple zeta correlation consistent basis sets for boron through neon, *J. Mol. Struct. THEOCHEM* **388**, 339 (1996).
- [22] S. Harrison and J. Tennyson, Bound and continuum states of molecular anions, *Journal of Physics B: Atomic, Molecular and Optical Physics*, 045206 (2011).
- [23] L. C. Chiu and M. Moharerrzadeh, Translational and rotational expansion of spherical gaussian wave functions for multicenter molecular integrals, *J. Chem. Phys.* **101**, 449 (1994), <https://doi.org/10.1063/1.468154>.
- [24] F. A. Gianturco and T. Stoecklin, Electron scattering from acetylene: elastic integral and differential cross sections at low energies, *J. Phys. B.* **27**, 5903 (1994).
- [25] F. Turpin, P. Halvick, and T. Stoecklin, The interaction of mnh with he : Ab initio potential energy surface and bound states, *J. Chem. Phys.* **132**, 214305 (2010).
- [26] C. Gottlieb, E. Gottlieb, P. Thaddeus, and H. Kawamura, Laboratory detection of the c_3n and c_4h free radicals, *Astrophys. J.* **275**, 916 (1983).
- [27] S. V. Jerosimić, M. Z. Milovanović, R. Wester, and F. A. Gianturco, Chapter three - dipole-bound states contribution to the formation of anionic carbonitriles in the ism: Calculations using multireference methods for c_3n^- , in *Rufus Ritchie, A Gentleman and A Scholar*, Advances in Quantum Chemistry, Vol. 80, edited by J. R. Sabin and J. Oddershede (Academic Press, 2019) pp. 47–86.
- [28] M. Ayouz, R. Lopes, M. Raoult, O. Dulieu, and V. Kokoouline, Formation of H_3^- by radiative association of H_2 and H^- in the interstellar medium, *Phys. Rev. A* **83**, 052712 (2011).
- [29] T. Stoecklin, F. Lique, and M. Hochlaf, A new theoretical method for calculating the radiative association cross section of a triatomic molecule: application to n_2-h^- , *Phys. Chem. Chem. Phys.* **15**, 13818 (2013).
- [30] N. Douguet, S. Fonseca dos Santos, M. Raoult, O. Dulieu, A. E. Orel, and V. Kokoouline, Theory of radiative electron attachment to molecules: Benchmark study of CN^- , *Phys. Rev. A* **88**, 052710 (2013).
- [31] N. Douguet, S. Fonseca dos Santos, M. Raoult, O. Dulieu, A. E. Orel, and V. Kokoouline, Theoretical study of radiative electron attachment to CN , C_2H , and C_4H radicals, *J. Chem. Phys.* **142**, 234309 (2015).
- [32] T. A. Yen, E. Garand, A. T. Shreve, and D. M. Neumark, Anion photoelectron spectroscopy of C_3N^- and C_5N^- , *J. Phys. Chem. A* **114**, 3215 (2010).
- [33] F. Carelli, F. A. Gianturco, R. Wester, and M. Satta, Formation of cyanopolyne anions in the interstellar medium: The possible role of permanent dipoles, *J. Chem. Phys.* **141**, 054302 (2014).
- [34] V. M. Bierbaum, Anions in space and in the laboratory, *Proceedings of the International Astronomical Union* **7**, 383–389 (2011).
- [35] M. Agúndez, J. Cernicharo, M. Guélin, C. Kahane, E. Roueff, J. Kłos, F. J. Aoiz, F. Lique, N. Marcelino, J. R. Goicoechea, M. G. García, C. A. Gottlieb, M. C. McCarthy, and P. Thaddeus, Astronomical identification

- of cn^- , the smallest observed molecular anion ^{***}, *A&A* **517**, L2 (2010).
- [36] Y. Liu, G.-Z. Zhu, D.-F. Yuan, C.-H. Qian, Y.-R. Zhang, B. M. Rubenstein, and L.-S. Wang, Observation of a symmetry-forbidden excited quadrupole-bound state, *J. Am. Chem. Soc.* **142**, 20240 (2020).